

Erosive Wear Study of the AISI 201LN Stainless Steel: A Comparison with the AISI 304 and AISI 410 Stainless Steels



ANA PAULA MARQUES DE OLIVEIRA, MANUEL HOUMARD,
WILIAN DA SILVA LABIAPARI, and CRISTINA GODOY

Synergistic corrosion and oxidation can accelerate the wear phenomenon in aggressive environments such as machinery operating in mining industries. The main purpose of this article is to study the erosion wear behavior of the AISI 201LN austenitic stainless steel toward an erosive wear process simulating the flow of particles in chutes. In addition to its good resistance to corrosion, the high Md temperature and low stacking fault energy (SFE) presented by the AISI 201LN steel favor its deformation-induced ϵ -martensitic transformation and, consequently, its work-hardening capacity. These characteristics induce a high potential in applications where mechanical wear occurs simultaneously with corrosion. For comparison purposes, AISI 304 and AISI 410 stainless steels, commonly used in mining and agroindustry equipment, were also studied in this work. Among the austenitic alloys, since its composition is weak in nickel, the AISI 201LN steel has a low production cost. The erosion tests were performed with impact angles of 20 and 90 deg, and the eroded samples were characterized by optical microscopy, scanning electron microscopy (SEM), and microhardness measurements. All the materials studied presented erosive wear by plastic deformation, and the AISI 201LN steel exhibited the highest erosive wear resistance. Its high ductility, high hardening rate, and high tendency to form martensite by deformation were fundamentals for such response. As a result, the AISI 201LN stainless steel seems promising as a cheaper material for applications in equipment that undergoes simultaneous erosive and corrosive wear.

<https://doi.org/10.1007/s11661-019-05123-1>

© The Minerals, Metals & Materials Society and ASM International 2019

I. INTRODUCTION

EROSIVE wear is caused by hard particles striking the surface, either carried by a gas stream or a liquid flow.^[1,2] It is a common phenomenon in mining and agroindustry processes, mainly where materials transfer

occurs (*e.g.*, chutes). In some parts of the chute equipment, the iron core particles flow, for example, strikes the equipment surface, applying a contact force during a long period of time, which leads to an erosive wear of the structural material used. The erosive wear intensity depends on the number, mass, velocity, and hardness of the individual particles striking the surface, as well as their impact velocity. These characteristics define the erosive wear problems.^[1,2] Several factors and parameters of the tribological system influence the erosion mechanism. Thus, the knowledge of the mechanical and metallurgical characteristics of the involved materials is fundamental for such a study.^[3]

The concern in studying stainless steels for applications in areas, such as mining and agroindustry, is that in addition to wear resistance, it is necessary to use materials that are resistant to corrosion due to the presence of humidity in these processes.^[4] In studies carried out by Aperam in the Valemix Mining Company,^[5] the performances of both AISI 410 and carbon steels were compared. In this work, the carbon steel with an initial thickness of 6 mm reaches, after 6 months of use, a thickness ranging from 1 to 3 mm, owing to a

ANA PAULA MARQUES DE OLIVEIRA is with the Department of Chemical Engineering, Federal University of Minas Gerais (UFMG), Avenida Presidente Antônio Carlos, 6627, Campus UFMG, Escola de Engenharia, bloco 2, 5° andar, Belo Horizonte, MG CEP: 31270-901, Brazil. Contact e-mail: p.anamarques@gmail.com
MANUEL HOUMARD is with the Department of Materials Engineering and Civil Construction, Federal University of Minas Gerais (UFMG), Avenida Presidente Antônio Carlos, 6627, Campus UFMG, Escola de Engenharia, bloco 1, sala 3304, Belo Horizonte, MG, CEP: 31270-901, Brazil. WILIAN DA SILVA LABIAPARI is with the R&D of Aperam South America, Praça 1° de Maio, 9, Centro, Timóteo MG CEP: 35.180-018, Brazil. CRISTINA GODOY is with the Department of Metallurgical Engineering and Materials, Federal University of Minas Gerais (UFMG), Avenida Presidente Antônio Carlos, 6627, Campus UFMG, bloco 1, sala 1804, Escola de Engenharia, Belo Horizonte, MG CEP: 31270-901, Brazil.

Manuscript submitted August 21, 2018.

Article published online January 31, 2019

severe wear in an environment combining the corrosion and abrasion phenomena. On the other hand, for AISI 410 stainless steel with an initial thickness of 4.75 mm, a reduction of only 0.3 mm has been observed. In this application, mechanical strength and good corrosion resistance enable a significant increase in durability, making the stainless steel highly competitive and the best alternative for such industrial applications. In addition, due to its higher mechanical resistance, smaller thicknesses are required. Thus, the expanded stainless steel sheets were processed with thicknesses about 30 pct lower than the carbon steel, ensuring the structural strength with an important reduction of cost. As a result, combined corrosion and wear resistances were demonstrated to be a great advantage of the stainless steel.^[5]

Two types of erosion wear mechanisms exist, the one by plastic deformation and the other one by fragile fracture.^[1] Generally, the first one is predominant for ductile materials and the second for fragile ones. However, the ductile and fragile terms should be used with caution, since the same material may present different mechanisms according to both processing characteristics and the tribological system. In erosive wear by fragile fracture, the material is removed from the surface by cracks formation and material shear. If the impact occurs perpendicularly to the surface direction, the impact energy is stronger, the crack propagates faster, and, consequently, the wear is higher than for shallow angles.^[1]

The erosion mechanism by plastic deformation proposes that when the erosive particle collides with the surface, the material displaces due to the particle penetration following three different behaviors. It could (1) be accommodated by elastic deformation; (2) form a crater because of the plastic deformation (mechanical conformation); and (3) have fragments removed by the impact, leading to a mass loss of the material and its wear. Higher wear by plastic deformation occurs for an angle near 20 or 30 deg because the erosive particles cause grooves on the material surface, which leads to the formation of protruding edges becoming fragility points.^[1] When other particles collide with the surface, these formed edges are removed as wear debris. Thus, the process is described by plastic deformation and loss of material by cutting occurring simultaneously.^[6,7] Erosive wear is extremely complex because it involves a diversity of parameters that exert direct influence on the process.^[8] In general, they can be subdivided into three groups: wear system, erosive particles, and eroded material parameters.

In this work, we present a comparison between the erosive wear of three stainless steels and the correlation of these results with their mechanical and metallurgical properties. The objective of the work is to study the influence of the stainless steel structures on their erosion resistance. The three chosen stainless steels are the ferritic AISI 410 steel and two austenitic stainless steels, AISI 304 and AISI 201LN. The latter is the main focus of the research, since it is a less studied material but with a high potential for future applications due to its high transformation-induced plasticity (TRIP) effect. For

Table I. Chemical Compositions (Mass Pct) of AISI 201LN, AISI 304, and AISI 410 Stainless Steels (Only the Principal Elements Are Presented)

Elements	AISI 201LN	AISI 304	AISI 410
Fe	71.168	71.202	87.270
C	0.033	0.019	0.015
Cr	17.001	18.1423	11.1143
Ni	4.0478	8.0448	0.3468
Mn	6.9646	1.3635	0.5233
Mo	0.0207	0.1317	0.0261
N	0.1506	0.0473	0.0184

such steels, a martensite transition occurs during plastic deformation at low temperature, increasing the work-hardening rate, the uniform ductility prior to necking, and its fracture toughness.^[9] This steel also presents a smaller production cost among the austenitic stainless steels, owing to its poorer chemical composition in nickel elements, and a good resistance to corrosion.^[10–12] AISI 304 and AISI 410 were chosen for comparison purposes because these materials are well known and commonly used in mining and agroindustry equipment.^[5]

II. MATERIALS AND METHODS

For the research, two austenitic stainless steels with TRIP effect, AISI 201LN and AISI 304, and ferritic stainless steel, AISI 410, were selected. The chemical composition of the studied materials is shown in Table I. They have been chosen to study the influence of the different structures on the erosive wear resistance.

Modifications were made in shot blasting equipment (CMV, model GS-9075X, series 002/1996) to adjust it for erosive wear tests. The experience parameters, such as erosive particles' flow, distance, and impact angle between the eroded substrate and the erosive particle gun, were controlled. In order to control the flow of erosive material and avoid its recirculation, an external silo was constructed. During the erosion test, the mass flow of erosive particle material remained constant at 2.0 kg/min. In addition to the silo, a support was built for the gun, allowing for control of the distance and the impact angle of the flow in relation to the sample position. The customized equipment used in this study is schematized in Figure 1.

The tests were performed with impact angles of 20 and 90 deg. The samples, with dimensions of 80 × 100 mm², were placed on a support to control the alignment with the erosive flow and its immobilization during the experiment. The distance between the erosive particle gun and samples was fixed to 20 mm. In all tests, compressed air pressure was kept constant at 6.0 × 10⁵ Pa. The density of the erosive particles was 7.4 ± 0.4 g/cm³ and the blast gun diameter was 7.1 mm. Thus, considering potential and kinetic energy present and an average velocity of the erosive particles of 0.114 m/s calculated from the parameters previously cited, the

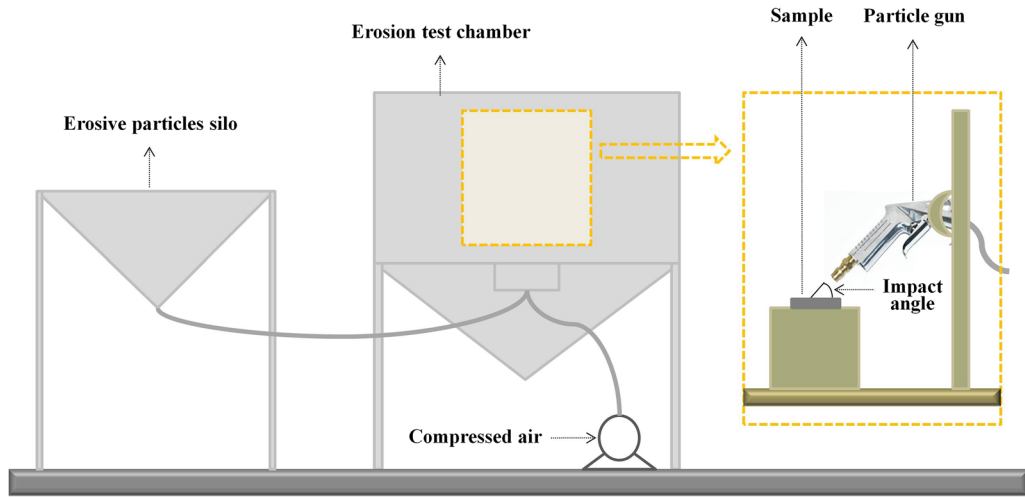


Fig. 1—Schema of the equipment adapted for the erosive wear tests performed in this work.

total energy involved in the process, divided by the mass of the erosive particles, can be estimated at 0.203 J/kg. Erosive wear rates were determined by the mass difference of the samples previously washed, sonicated for 5 minutes in ethanol, and then dried. The tests were performed in triplicate.

Erosive particles and sample structures were analyzed by optical microscopy (Buehler, Simplimet 1000 model) and scanning electron microscopy (SEM, Oxford, 7509 A4 model, 161-5350-TV5-2614 series, 500 V). Chemical attacks were adequately used to prepare the sample surfaces before the optical characterizations. The standard etchants Nital (2 wt pct of nitric acid in methanol) and Behara (20-mL HCl, 80-mL H₂O, and 0.30 g of potassium metabisulfite) were used to reveal the martensite phase, and the grain structure was revealed by etching in Vilella's solution (1-g picric acid, 5-mL hydrochloric acid, and 100-mL ethanol). In addition, mechanical tests were carried out in agreement with the ASTM A370-12 norm,^[13] using a universal traction machine (Instron, model 5583, with a maximum load capacity of 150 kN). Five samples were tested for each studied material. From these measurements, the hardening coefficient (n) was calculated from Eq. [1], relating true stress (σ_V) with true deformation (ϵ_V) during the plastic deformation.^[14]

$$\sigma_V = K \cdot (\epsilon_V)^n \quad [1]$$

Finally, the microhardness measurements fulfilled after the erosion tests were performed by using a microdurometer Future Tec FM 700 with a load of 0.5 N.

III. RESULTS AND DISCUSSION

A. Erosive Particle Characterization

There is unanimity in the literature that some erosive particle factors, such as morphology, hardness, and size, have a direct influence on erosion rates.^[15–18] In this

way, all these parameters were previously evaluated to guarantee the homogeneity, reproducibility, and representativity of the results.^[19] In this work, quenched AISI 1080 carbon steel shot was used as erosive particles. The granulometric characterization was done by using a laser granulometry technique (Cilas granulometer, model 1064). The result shows a uniform distribution of particles with an average diameter of $403.8 \pm 4.9 \mu\text{m}$ (Figure 2). Then, the erosive particles were observed by optical microscopy. Figure 3 shows clearly that the erosive particles are spherical with a uniform diameter and a typical fine and homogeneous martensitic microstructure.

B. As-Received Stainless Steels Characterization

As mentioned in the methodology, tensile tests were carried out to characterize the mechanical properties of the studied materials. Examples of typical true stress–strain curves for the AISI 201LN, AISI 304, and AISI 410 stainless steel obtained in this work are shown in Figure 4. The strain-hardening exponent (n) was obtained by analyzing these true stress–strain curves during the plastic deformation; the results are present in the insert of Figure 4. These values indicate a higher tendency for the AISI 201LN to be hardened in relation to the AISI 304 and AISI 410 steels. Besides, the total plastic deformation is higher for austenitic steels (AISI 201 and AISI 304 steels) than the ferritic one (AISI 410 steel).

In order to compare the stability of austenite in AISI 201LN and AISI 304 steels, the stacking fault energies (SFEs) and Md_{30} (temperature for 50 pct of martensite transformation after a true deformation of 0.3) of these materials were calculated by using the models proposed by Schramm and Reed (Eq. [2])^[20] and Nohara (Eq. [3]), where d represents the ASTM austenite grain,^[21] respectively. The results are described in Table II. The higher value of Md_{30} and lower SFE presented by the AISI 201LN steel, in relation to the AISI 304, confirm a

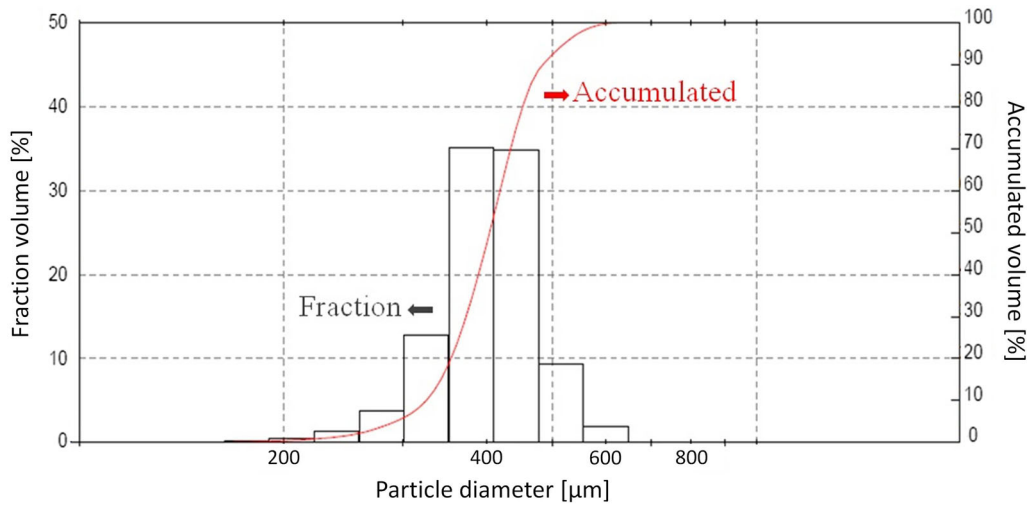


Fig. 2—Granulometric analysis of the erosive particles used in the erosion wear tests.

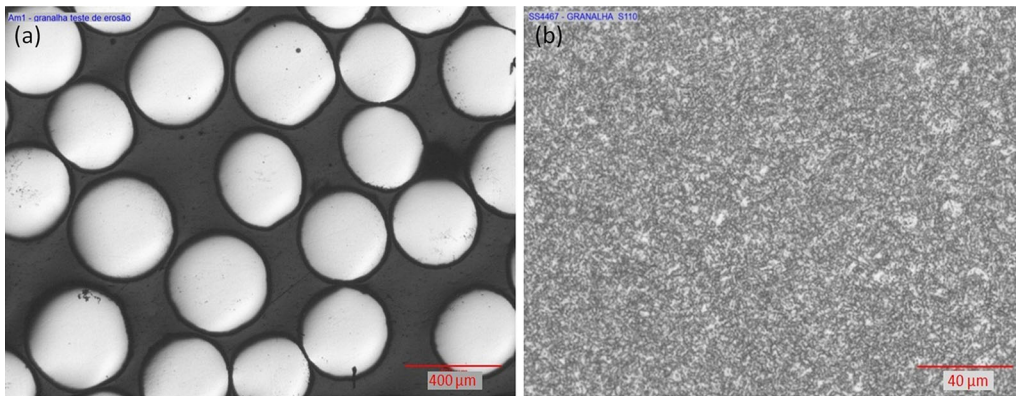


Fig. 3—Structure of the erosive particles used in the wear tests. (a) Optical microscopy to observe the shape (without chemical attack). (b) Optical microscopy to identify the martensitic microstructure (chemical attack: Nital).

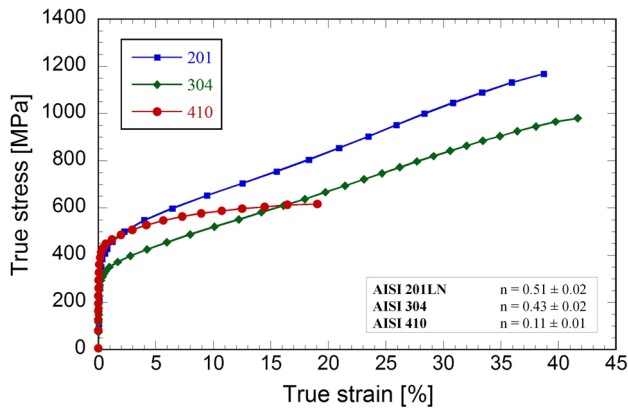


Fig. 4—Examples of true stress–strain curves of AISI 201LN and 304 austenitic stainless steels and AISI 410 ferritic stainless steel. Strain-hardening exponents (n) calculated from all the true stress–strain curves are present in the insert.

lower austenite stability and, consequently, a higher tendency to form martensite by deformation (TRIP effect).^[22]

$$\text{EFE} \left(\frac{\text{mJ}}{\text{m}^2} \right) = -53 + 6.2(\text{pct Ni}) + 0.7(\text{pct Cr}) + 3.2(\text{pct Mn}) + 9.3(\text{pct Mo}) \quad [2]$$

$$M_{d30} (^{\circ}\text{C}) = 551 - [462(\text{pct C} + \text{pct N}) + 9.2(\text{pct Si}) + 8.1(\text{pct Mn}) + 13.7(\text{pct Cr}) + 29(\text{pct Ni} + \text{pct Cu}) + 18.5(\text{pct Mo}) + 68(\text{pct Nb}) + 142(d - 8)] \quad [3]$$

C. Erosive Wear Comparison

Figure 5 exhibits the mass loss of the studied materials as a function of the erosion time for incidence angles of 20 and 90 deg. In all cases, higher erosions are observed for a shallow angle, which is an indication that the wear mechanism by plastic deformation occurred.^[1]

In the literature, it is clear that debris removal is dependent on the impact angle. Rupture of the crater edges formed by the material displacement occurs at 20 deg. For the normal angle, the deformation is deeper and fewer edges form; thus, more impacts are necessary to remove each fragment of debris. In this condition, the material will undergo more cycles of plastic deformation until debris removal. This proposed mechanism is clearly evidenced in Figure 6, which illustrates optical microscopy images of the AISI 410 steel as an example.

Table II. Md_{30} and SFE Values, Respectively, Calculated from the Nohara^[21] and Schramm and Reed^[20] Equations for the AISI 201LN and AISI 304 Austenitic Stainless Steels

Material	SFE (mJ/m ²)	Md_{30} (°C)
AISI 201LN	6.5	55
AISI 304	15.2	12.9

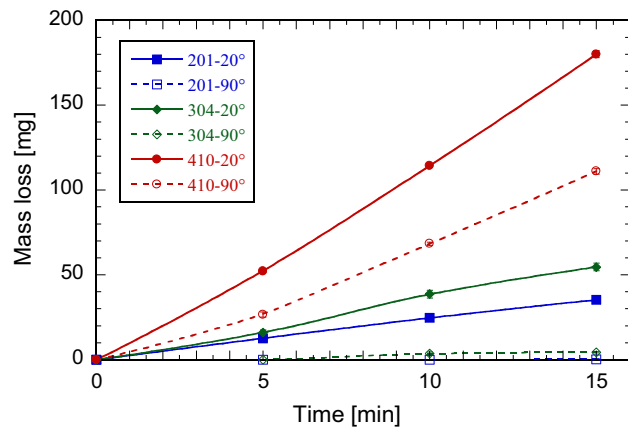


Fig. 5—Mass loss as a function of the erosive wear time at impact angles of 20 deg (continuous line) and 90 deg (dotted line) for AISI 201LN, AISI 304, and AISI 410 stainless steel. The fit lines are used only as a guide for the eyes.

It is possible to observe that for an impact angle of 90 deg, the plastic deformation is deeper than for 20 deg. For the normal angle, the material is deeply more compacted than for a shallow angle. In the latter case, it is swept and cut along the eroded surface. Figure 6(a) illustrates the presence of superficial cracks (indicated by an arrow) that probably led to the higher loss of material at 20 deg, evidenced in Figure 6.

Erosion rates, E , which represent the ratio of the mass of material removed by the mass of erosive particles that knocks against the surface were calculated from Figure 5 and are shown in Table III. The erosion rate in the steady state is characterized as a linear relationship between the mass of material removed by the mass of erosive particles. Thus, for constant erosive particle flow, the erosion rate stays constant along the erosion time. In Figure 5, a period of “running” can be observed during the first minutes in which the evolution of the removed material mass as a function of time presents a nonlinear behavior. After a time, a permanent erosion state seems to be reached in agreement to reported work.^[23] This running period has not been specifically studied in this work, but it can be observed approximately in the first 5 minutes of the erosion experiment. As a consequence, E was calculated considering the mass loss between the time of 5 and 15 minutes using a constant erosive particle mass flow of 2 kg/min.

For both angles tested, the wear rate suffered by the AISI 410 steel was higher, followed by AISI 304, and finally AISI 201LN, which presented the highest wear resistance of the studied materials. Erosive wear by plastic deformation is commonly discussed to be

Table III. Erosion Linear Coefficients, E ($\times 10^{-6}$ g/g), of AISI 201LN, AISI 304, and AISI 410 Stainless Steels at 20 and 90 Deg Impact Angles

Material	E ($\times 10^{-6}$) Impact Angle: 20 Deg	E ($\times 10^{-6}$) Impact Angle: 90 Deg
AISI 201LN	1.227 ± 0.026	0.011 ± 0.010
AISI 304	1.787 ± 0.098	0.110 ± 0.056
AISI 410	5.655 ± 0.224	3.264 ± 0.309

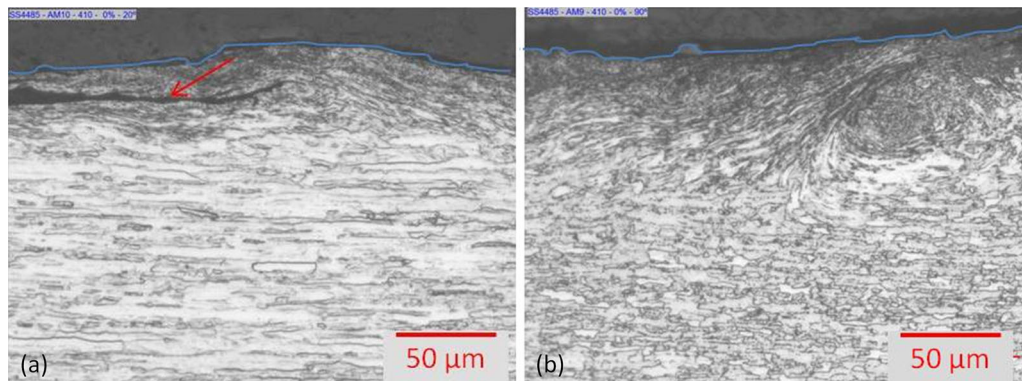


Fig. 6—Micrographs along the thickness of AISI 410 steel after erosive wear testing for impact angles of (a) 20 deg and (b) 90 deg. Chemical attack: Vilella. The arrow indicates superficial cracks. The blue lines indicate the external surface of the samples.

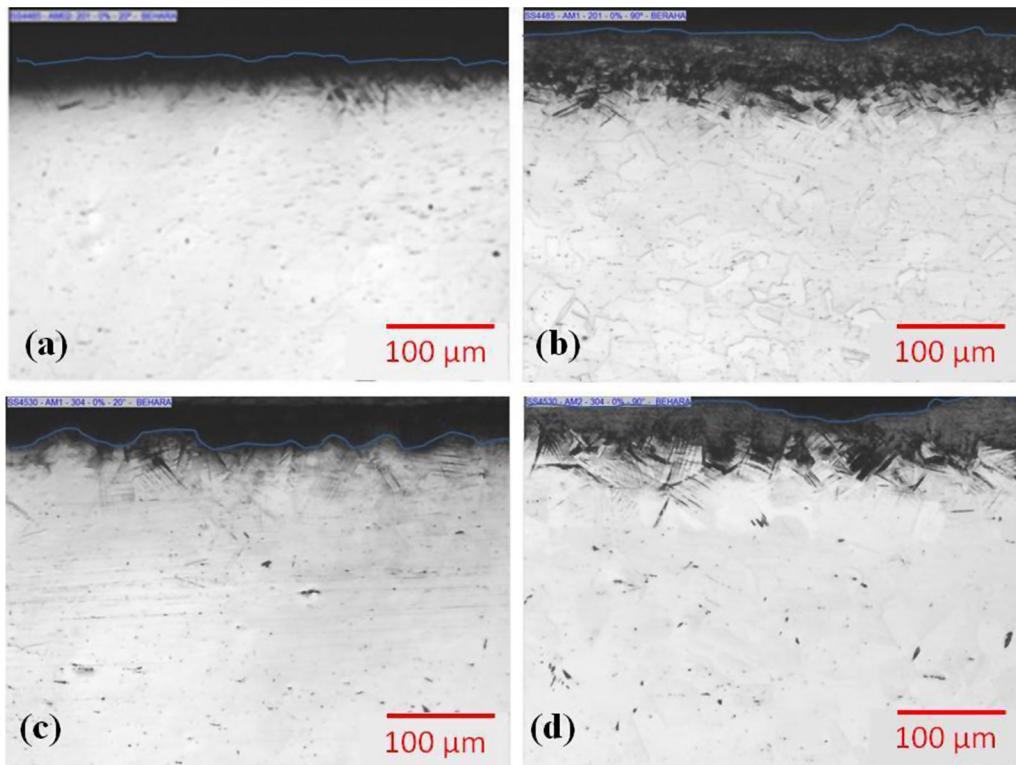


Fig. 7—Micrographs along the thickness of the AISI 201LN and AISI 304 steels after erosive wear with impact angles of 20 and 90 deg. (a) AISI 201-20 deg, (b) AISI 201-90 deg, (c) AISI 304-20 deg, and (d) AISI 304-90 deg. Chemical attack: Behara. The blue lines indicate the external surface of the samples.

inversely proportional to the studied material hardness. However, since the surface is hardened by plastic deformation during the successive particle impacts, it seems more consistent to correlate the erosion rate with the deformed surface hardness rather than considering the initial hardness of the material.^[1] Due to its bcc crystalline structure, the ferritic steel AISI 410 deformed only moderately with cold working and, consequently, did not experience significant hardening. On the other hand, stainless steels AISI 201LN and AISI 304 are austenitic with an fcc crystalline structure. Thus, they have higher ductility as well as presenting a TRIP effect.^[22,24,25] As a result, although the AISI 410 steel has a high initial resistance compared to the others, its smaller strain-hardening exponent (Figure 4) contributes to the lower erosion resistance observed for this material during the erosion tests.

Another important parameter is the lower ductility of the AISI 410 shown in Figure 4 from the tensile test curves. Indeed, such a characteristic induces a higher erosive wear rate due to a lower capacity to support plastic deformation.^[26–28] Thus, for the same erosion time, since it has less capacity to withstand deformations and smaller strain hardening, the AISI 410 steel will form more debris than the others and its wear will be more intense. However, all materials, including the AISI 410 steel, underwent a plastic deformation mechanism, confirmed by a greater erosion resistance toward the 90 deg angle. Considering the area under the stress–strain curves representing the work necessary to break a unity

of the tested material volume, Figure 4 indicates that the AISI 410 stainless steel also had a lower toughness, reducing its capacity to withstand impacts and somehow contributing to premature fragile fractures. Finally, all mentioned parameters act together during the erosion wear and justify that the tribological system must be considered as a whole.^[29–31] In other words, erosive wear resistance or fragility cannot be related to a single parameter. Thus, these mentioned factors help in understanding the higher wear suffered by the AISI 410 steel in relation to the other steels studied in this work.

Both austenitic steels studied here present a TRIP effect, so they have a great hardening of the surface due to the impact stresses caused by the erosive particles' impacts.^[32] These steels were hardened by the austenite–martensite transformation induced by cold deformation, which does not occur for the AISI 410 ferritic steel. The AISI 201LN and AISI 304 steels, despite having a similar structure, have a significant difference in erosive wear rates (Table III), which is also a very relevant point of this study. Indeed, the erosive wear resistance is higher for the AISI 201LN steel than for the AISI 304 one in the erosion tests performed. Microscopy images demonstrate that the AISI 201LN steel presented a deeper and more compact martensite transformation induced by plasticity than the AISI 304 steel (Figure 7). Such results are in agreement with the facts that the AISI 201LN steel has lower SFE and higher Md_{30} , which represents a higher tendency to form martensite in

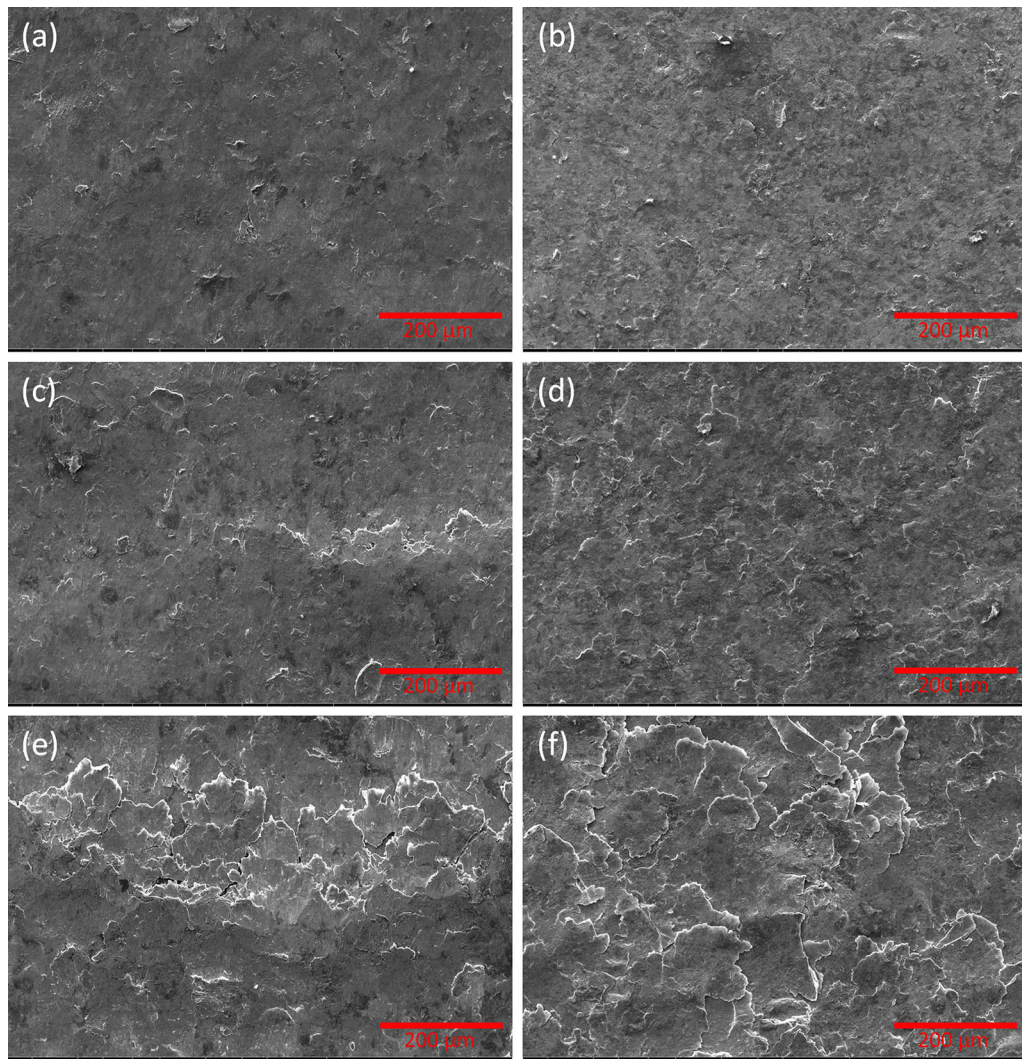


Fig. 8—SEM analyses of the eroded surfaces with impact angles of 20 and 90 deg: (a) AISI 201LN-20 deg, (b) AISI 201LN-90 deg, (c) AISI 304-20 deg, (d) AISI 304-90 deg, (e) AISI 410-20 deg, and (f) AISI 410-90 deg.

its structure.^[6,33,34] Its chemical composition presents fewer alloy elements, especially Ni and Cr, than the AISI 304 austenitic steel, which increases its Md_{30} according to Eq. [3]. Thermodynamically, a higher Md_{30} means that the transformation of austenite to martensite by plastic deformation is more favorable.^[20] Indeed, the presence of such an element in a substitutional position creates stresses in the fcc austenite structure, which makes the simultaneous dislocation of the atoms leading to the martensite formation more difficult. This characteristic contributes positively to increased erosion resistance, storing more energy during the transformation and, consequently, absorbing more impact energy. This hard martensite phase formed during the erosion tests acts as a barrier to the erosive particles' penetration.^[4,35,36] It is important to emphasize that the sublayers, *i.e.*, the bulk material, will continue to be austenitic, retaining their ductility, which is also indispensable to limiting the wear process.

D. Eroded Sample Characterization

Figure 8 shows the SEM images of the crater surfaces after erosive wear. For all three stainless steels studied here, despite a smaller erosion rate for 20 deg, images show higher degradation of the eroded surfaces for impact angles of 90 deg than for 20 deg. Especially, since it presented a higher wear rate, this observation is more evident for the AISI 410 material. In fact, for an impact angle of 20 deg, the material is swept by the edge of the erosive particle, whereas at 90 deg, debris formation occurs at higher fracture intensity, which requires a greater critical deformation to reach this fracture stress, leading to a lower mass loss but a high local plastic deformation.

In order to evaluate the hardening effect by work hardening and martensite phase transformation, microhardness measurements were performed along the thickness of the materials from their eroded surfaces.

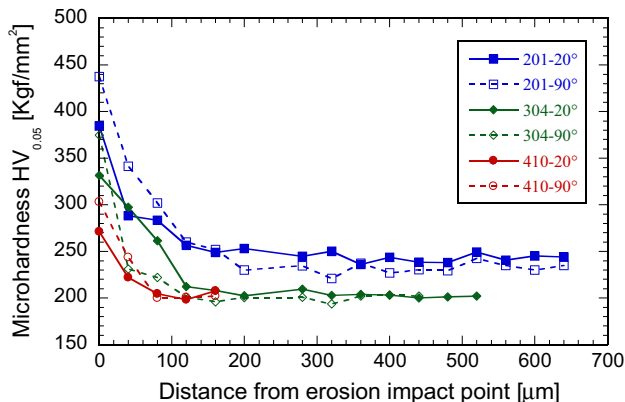


Fig. 9—Vickers microhardness along the thickness of the AISI 201LN, AISI 304, and AISI 410 steels measured in the crater formed during the erosive wear at impact angles of 20 deg (continuous line) and 90 deg (dotted line).

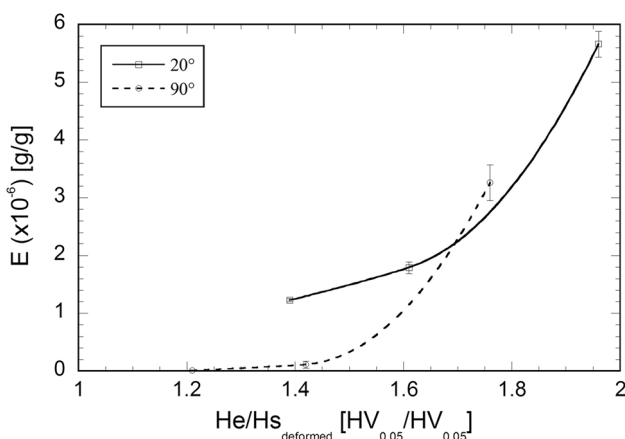


Fig. 10—Correlation between the erosive wear rate E and the hardness of the erosive particle (He) divided by the hardness of the deformed surface ($Hs_{deformed}$), at impact angles of 20 and 90 deg, for AISI 201LN, AISI 304, and AISI 410 steels. The fit lines are used only as a guide for the eyes.

The results are shown in Figure 9. For the AISI 410 steel, only a slight hardening occurred due to grain deformation. This behavior contributes to the low erosive resistance of this material, as previously discussed. Another relevant point to be analyzed is that the hardening of the AISI 201LN steel, evidenced by the increased hardness measured at the center of the crater after the erosion tests (*i.e.*, a distance from erosion impact point null), was higher than the AISI 304 one, which seems to confirm the higher formation of martensite and surface work hardening of this material during the erosive wear, as previously discussed.

Figure 10 shows the correlation between the erosive wear rate and the hardness of the erosive particle (He) divided by the hardness of the deformed surface ($Hs_{deformed}$) in the center of the crater formed during the erosion tests, at impact angles of 20 and 90 deg, for the three materials studied. It is clear that when the deformed surface has a higher final hardness, *i.e.*, a smaller $He/Hs_{deformed}$, a higher resistance to erosive

Table IV. Erosion Linear Coefficients, E [$\times 10^{-6}$ g/g], Divided by the Eroded Area (cm^2) of AISI 201LN, AISI 304, and AISI 410 Stainless Steels at 20 and 90 Deg Impact Angles

Material	E ($\times 10^{-6}$)/Area (cm^2) Impact Angle: 20 Deg	E ($\times 10^{-6}$)/Area (cm^2) Impact Angle: 90 Deg
AISI 201LN	0.030 ± 0.001	0.031 ± 0.008
AISI 304	0.045 ± 0.002	0.245 ± 0.125
AISI 410	0.141 ± 0.006	7.245 ± 0.686

wear is obtained. Thus, materials with high hardening tend to have a lower erosive wear rate. As previously mentioned, the wear is smaller for an impact angle of 90 deg because fewer edges are formed, and, consequently, a smaller mass loss, during the wear process.

Finally, it is important to describe that for an angle of 20 deg, the wear phenomenon is shallower but affects wider areas of the surface materials. Thus, although a higher debris formation occurs at a shallow angle, the material may fail first when the flow erosive is perpendicular to the material surface due to the higher localized plastic deformation, leading to a higher located loss of material, which is in agreement with the observation about Figure 8. Table IV presents the erosive wear rate divided by the eroded area for the three materials studied in this work. Although the erosive wear rate is lower for an angle of 90 deg, when these data are normalized by the eroded area, *i.e.*, the area affected by the wear, an opposite behavior is observed. Such results confirm that the wear process with normal impact angle has to be avoided in industrial applications.

IV. CONCLUSIONS

All of the materials studied presented erosive wear by the plastic deformation mechanism with a higher mass loss for a shallow angle. However, the observed wear degradation seemed to be more located for normal impact, which could lead the material to fail faster in such a situation. Among the materials studied, AISI 410 steel presented the lowest erosive wear resistance. Its low ductility, weak hardening rate, and nonformation of martensite by deformation were fundamental for this behavior. In relation to the austenitic stainless steels, AISI 201LN presented higher resistance to erosive wear than AISI 304 did. The higher value of Md_{30} and lower SFE presented by AISI 201LN indicate a lower austenite stability and, consequently, a higher tendency to form martensite by deformation to improve wear resistance. As a result, AISI 201LN, which is cheaper than austenite AISI 304, appears as a promising material for applications in equipment that could undergo simultaneous erosive and corrosive wear.

ACKNOWLEDGMENTS

The authors thank CAPES, FAPEMIG, and APERAM South America for financial support.

REFERENCES

1. Hutchings and S. Philip: *Tribology—Friction and Wear of Engineering Materials*, 2nd ed., Butterworth-Heinemann, Cambridge, UK, 2017.
2. R. Bellman and A. Levy: *Wear*, 1981, vol. 70, pp. 1–27.
3. M. Bingley and D. O’Flynn: *Wear*, 2005, vol. 258, pp. 511–25.
4. C. Allen and A. Ball: *Tribol. Int.*, 1996, vol. 29, pp. 105–16.
5. Aperam South America: Mining Plate (2016), <http://brasil.aperam.com/chapa-da-mineracao/>, <https://www.youtube.com/watch?v=NvLozFs-RF0> (in Portuguese). Accessed July 24, 2018.
6. J.G.A. Bitter: *Wear*, 1963, vol. 6, pp. 5–21.
7. J.G.A. Bitter: *Wear*, 1963, vol. 6, pp. 169–90.
8. G. Yadav, S. Tiwari, A. Rajput, R. Jatola, and M.L. Jain: “A Review: Erosion Wear Models,” *Int. Conf. Emerging Trends in Mechanical Engineering “ICETME,”* May 27–28, 2016.
9. R.W.K. Honeycombe: *Steels: Microstructure and Properties*, Edward Arnold, Lincoln University, Oxford, PA, 1982.
10. M. Tavares and J. Pardal: *Mater. Charact.*, 2009, vol. 60, pp. 907–11.
11. W. Chuaiphan and L. Srijaroenpramong: *J. Mater. Process. Technol.*, 2014, vol. 214, pp. 402–08.
12. J. Charles, J.D. Mithieux, J. Krautschick, N. Suutala, J.A. Simón, B. Van Hecke, and T. Pauly: *Rev. Metall. Int. J. Metall.*, 2009, vol. 106, pp. 90–98.
13. ASTM—American Standard for Testing Materials: “Standard Test Methods and Definitions for Mechanical Testing of Steel Products,” A370–12, ASTM International, West Conshohocken, PA, 2012.
14. W.D. Callister and D.G. Rethwisch: *Materials Science and Engineering*, 8th ed., Wiley, New York, NY, 2011.
15. M. Vite-Torres, J.R. Laguna-Camacho, R.E. Baldenebro-Castillo, E.A. Gallardo Hernández, E.E. Vera-Cárdena, and J. Vite-Torres: *Wear*, 2013, vol. 301, pp. 383–89.
16. M. Liebhart and A. Levy: *Wear*, 1991, vol. 151, pp. 381–90.
17. H. Clark and R.B. Hartwich: *Wear*, 2001, vol. 248, pp. 147–61.
18. A.V. Levy and P. Chik: *Wear*, 1983, vol. 89, pp. 151–62.
19. B.K. Gandhi, S.N. Singh, and V. Seshadri: *Tribol. Int.*, 1999, vol. 32, pp. 275–82.
20. T.E. Schramm and R.P. Reed: *Metall. Trans. A*, 1975, vol. 6A, pp. 1345–51.
21. K. Nohara, O. Yutaka, and O. Nobuo: *Tetsu-to-Hagané*, 1977, vol. 63, pp. 772–82.
22. C. Gauss, I.R. Souza Filho, M.J.R. Sandim, P.A. Suzuki, A.J. Ramirez, and H.R.Z. Sandim: *Mater. Sci. Eng. A*, 2016, vol. 651, pp. 507–16.
23. C. Viafara and A. Sinatora: *J. Mater. Prod. Technol.*, 2010, vol. 38, pp. 93–116.
24. F.T. Lischka and C.A.S. de Oliveira: *J. Achiev. Mater. Manufact. Eng.*, 2015, vol. 71, pp. 34–38.
25. Kovalev, A. Jahn, A. Weib, and P.R. Scheller: *Steel Res. Int.*, 2011, vol. 82, pp. 45–50.
26. A.V. Levy: *Wear*, 1986, vol. 108, pp. 1–21.
27. I. Finnie: *Wear*, 1972, vol. 19, pp. 81–90.
28. C.H. Chen, C.J. Altstetter, and J.M. Rigsbee: *Metall. Trans. A*, 1984, vol. 15A, pp. 719–28.
29. G. Sundararajan: *Metals*, 1983, vol. 36, pp. 474–95.
30. G.P. Tilly: *Wear*, 1973, vol. 23, pp. 87–96.
31. K.H. Zum Gahr: *Tribol. Ser.*, 1987, vol. 10, p. 560.
32. D. Hennessy, G. Steckel, and C. Altstetter: *Metall. Trans. A*, 1976, vol. 7A, pp. 415–24.
33. H. Pinto: Thesis, Technische Universität Berlin, Berlin, 2005, p. 53.
34. C.B. Post and W.S. Eberly: *Trans. ASM*, 1947, vol. 39, pp. 868–90.
35. D. Lopez, N.A. Falleiros, and A.P. Tschiptschin: *Tribol. Int.*, 2011, vol. 44, pp. 610–16.
36. R.J.K. Wood, J.C. Walker, T.J. Harvey, S. Wang, and S.S. Rajahram: *Wear*, 2013, vol. 306, pp. 254–62.